3D non-linear finite element analysis of a prestressed post-tensioned I-girder

Hokkaido University ○ Student Member Deepti SHARMA
Central South University Pengru DENG
Hokkaido University Member Takashi MATSUMOTO

1. INTRODUCTION

Transit infrastructure is one of the key components for the growth and sustained development of India. There are approximately 140,919 bridges in Indian Railways, with approximately 40.58% of them being over 60 years old [1].

Prestressed concrete (PSC) structures offer great advantages as compared to conventional ordinary reinforced concrete structures in terms of bridging long spans, controlled deflections, economical design, etc[2]. Because of the aforementioned advantages, PSC girder bridges are most common in practice. However, there have been a series of failures of PSC bridges all over the world, such as the sudden collapse of the Saint Stefano bridge in Italy in March 1999 and the pedestrian bridge at Lowe's Motor Speedway in North Carolina in 2000[3].

PSC girders undergo various damages in service due to corrosion, vehicular impact, etc. The estimation of residual strength after physical inspection of these damages is very important in view of public safety. Moreover, decisions regarding repair methodologies and retrofitting techniques also need information regarding the present health of the damaged girder. Finite Element Analysis (FEA) is one of the most cost-effective methods for structural health assessment. The behavior of corroded PSC girders has been evaluated using 1D and 2D FE analyses [4]. 3D detailed modeling accurately approximates the response of reinforced concrete structures. Smeared, discrete, and embedded modeling are the three approaches of reinforcement modeling in a 3D RC model [5]. Smeared and discrete formulations are unsuitable for complicated reinforcement. An embedded model, on the other hand, can represent the exact geometries of the reinforcement grid without changing the actual rebar arrangement to conform to the concrete FE mesh [6]. The present study aims at 3D solid modeling of a prestressed concrete girder using MSC Marc.

2. METHODOLOGY

In the present study, an existing railway prestressed post-tensioned girder bridge has been selected, and its nonlinear finite element analysis has been done using MSC Marc.

2.1. Geometrical details

The schematic layout geometry of the girder is shown in **Figure 1**. Solid element type-7 has been used for concrete and support steel plates. It is an eight-node, iso-parametric, hexahedral element, as shown in **Figure 2** (a). Truss element type-9 has been used for prestressing and reinforcing steel. It is a two-node, straight truss element, as shown in **Figure 2** (b). Embedded modeling has been used because of the complex reinforcement and curved tendon. Truss elements have been embedded into solid concrete elements using the INSERT function of MSC Marc, as shown in **Figure 2** (c). A quarter model has been used for the analysis as the geometry of the girder is symmetric about two planes.

2.2. Material properties

There are two grades of concrete used. For I girder and deck slab, concrete having characteristic cube compressive strengths of 50 MPa and 35 MPa, respectively, has been used. An empirical stress-strain model has been used for concrete in compression[7] and concrete in tension[8], as shown in **Figure 3** (a). A shear retention factor of 0.4 has been used[9]. Stress-relieved 7-wire strands (ASTM A416) Grade 260 have been used.

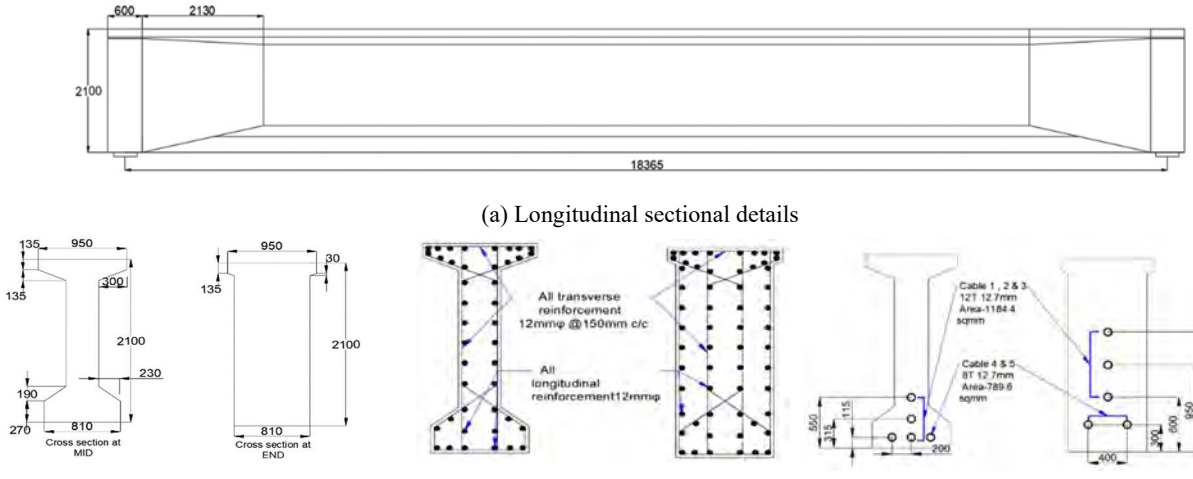

(a) Longitudinal sectional details

(b) Cross sectional details (c)Longitudinal and transverse reinforcement (d) Tendon arrangement

Figure 1 Girder configuration (all dimensions in mm)

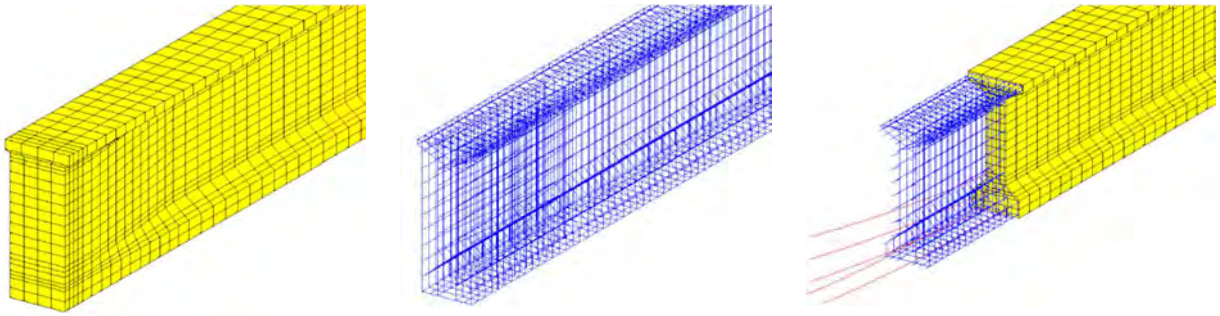

(a) Concrete (b) Reinforcing steel (c) Embedded model showing embedded prestressing & reinforcing steel

Figure 2 Girder geometry modelled in MSC Marc

(a) High strength concrete in compression and tension (b) Prestressing steel

Figure 3 Constitutive models

Table 1 Material properties of concrete and prestressing steel

Description of property	Elastic modulus (GPa)	Characteristic strength (MPa)	Ultimate stress (MPa)	Poisson's ratio	Cracking stress (MPa)	Ultimate strain	Yield stress (MPa)
I girder	36.7	50	-	0.2	4.95	0.003	-
Deck slab	36.7	35	-	0.2	4.141	0.003	-
Prestressing steel	186	-	1860	0.3	-	0.04	1674

A stress-strain relationship based on a modified power law formula[10] has been used for prestressing steel, as shown in **Figure 3** (b). The properties of concrete and prestressing steel are shown in **Table 1**. A bilinear stress-strain curve for reinforcing steel has been used with a yield stress of 415 MPa, an elastic modulus of 200 GPa, a poisson's ratio of 0.3, and a hardening modulus of 5630 MPa.

2.3. Field instrumentation

The girder has been equipped with optical strain sensors at the middle, intermediate, and end of the girder on the reinforcement near the top and bottom fibers. IIT Roorkee performed the instrumentation, which was funded by the Indian Railways.

2.4. Boundary conditions

The girder has been simply supported at the ends. The symmetric boundary conditions on the quarter model have been applied by fixing the translation degree of freedom perpendicular to the plane of symmetry. The number of elements has been reduced from 22,546 to 5,820 from the full model to the quarter model.

Table 2 Magnitude of load and method of application

Description of load	Nature of application	Magnitude
Self-weight	Gravity load	I girder -552 kN Deck slab -360 kN
Prestressing force	Thermal load	Cable 1, 2 & 3 -1653.3 kN Cable 4 & 5 -1102.2 kN
Load test	Face load	55 blocks weighing 8.5 tonne each.

2.5. Loading configuration

Many researchers have used thermal load, which is equivalent to prestressing force, to simulate the prestressing effect [11]. Likewise, in the present study, pre-stressing force is simulated in terms of a reduction in temperature. The girder has been sequentially loaded with self-weight (SW), first stage prestressing (FSP), superimposed dead load (SDL), second stage prestressing (SSP), and load test (LT) in order. Details about loading are shown in **Table 2**.

3. RESULTS AND DISCUSSIONS

3.1. Midspan displacement

The deflection response under each load has been evaluated as shown in **Figure 4**. The downward deflection under vertical

loads is less than the designed values. The upward deflection caused by the prestressing effect exceeds the prescribed limit. The prestressing effect has two components: axial compression due to the direct load and a hogging bending moment due to the eccentricity of the prestressing strands. It seems the prestressing effect due to the eccentricity of the strands dominates when simulation of the prestressing effect using thermal load has been done. Moreover, there are losses due to elastic shortening, friction, and curvature effects that are not accounted for in the simulation.

3.2. Bending stresses at midspan

The state of stress in the girder at various stages of loading is shown in **Figure 5**. Stress blocks are drawn at the girder's middle, intermediate, and end locations. Tensile stresses were only present in load case 1 (i.e., under SW+FSP). The magnitude of the maximum tensile stress was 0.1 MPa at the top fiber in the middle of the girder. whereas a maximum compressive stress of 13 MPa has been observed at the bottom fiber under load case 3 (SW+FSP+SDL+SSP). Both tensile and compressive stresses are below the permissible stress mentioned in **Table 3**.

3.3. Bending strains at midspan

Bending strains obtained at midspan have been compared with strains recorded using optical strain sensors. **Figure 6** shows the top fiber strain. Under vertical loads (SW, SDL, and LT), compressive strains have been observed, which are close to the instrumentation results. Under prestressing loads, tensile strains have been observed, whereas instrumentation results show compressive strains. Approximations in modeling, the omission of short-term losses, and the use of thermal load may have caused these discrepancies. **Figure 7** shows the bottom fiber strain. Tensile strains were observed under vertical loads, while compressive strains were observed under prestressing loads. The results are close to field values with a similar nature.

3.4. Bending stress along the longitudinal axis

Bending stresses were calculated analytically by superimposing axial compressive stress, bending stresses due to prestressing force, and bending stresses due to vertical loads. They are compared with FEM and instrumentation results, as shown in **Figure 8**. Because the FE model is normally stiffer than the real structure, FEM results are less than analytical results for all load cases. **Figure 8** (a) shows bending stress under SW. Instrumentation results fall in between analytical and FEM results. **Figure 8** (b) shows bending stress under the FSP. Field results show compressive stresses against tensile stresses as per the analytical calculations and FEM results at the top. The magnitude of compressive stresses in the field results is higher than the analytical and FEM results at the bottom. Discrepancies may be due to the simulation of prestressing loads using thermal strain. SSP shows a similar trend as shown in **Figure 8** (c). **Figure 8** (d) shows bending stress under the LT. Bending stresses at the top fiber are close to FEM results, whereas at the bottom fiber, they lie in between FEM and analytical results.

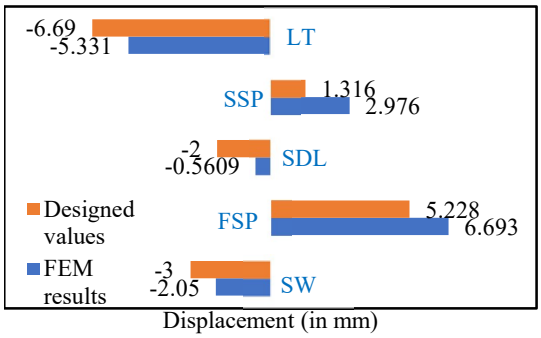

Figure 4 Midspan displacement

Table 3 Permissible stresses in concrete (in MPa)

	Compression	Tension
At FSP	-20	+2
At SSP	-25	+2.5
At Service	-16.5	0

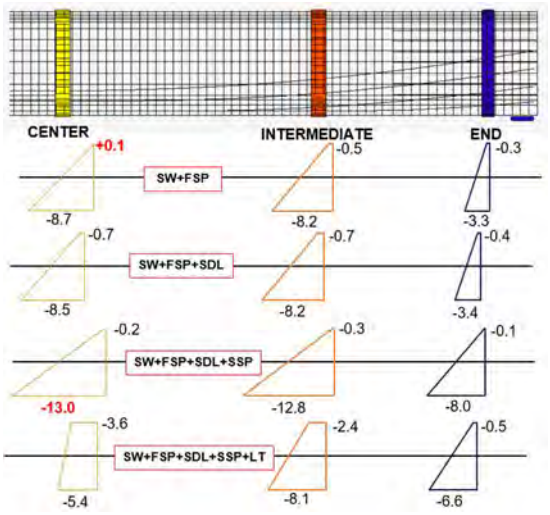

Figure 5 Bending stress under various load cases. (in MPa)

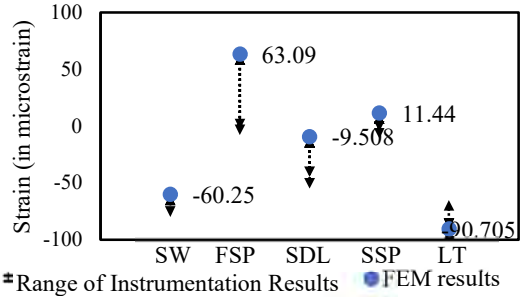

Figure 6 Top fiber strain comparison at midspan

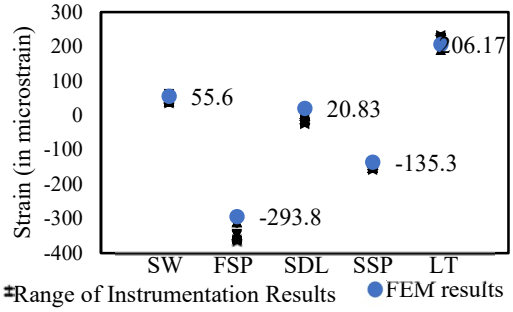

Figure 7 Bottom fiber strain comparison at midspan

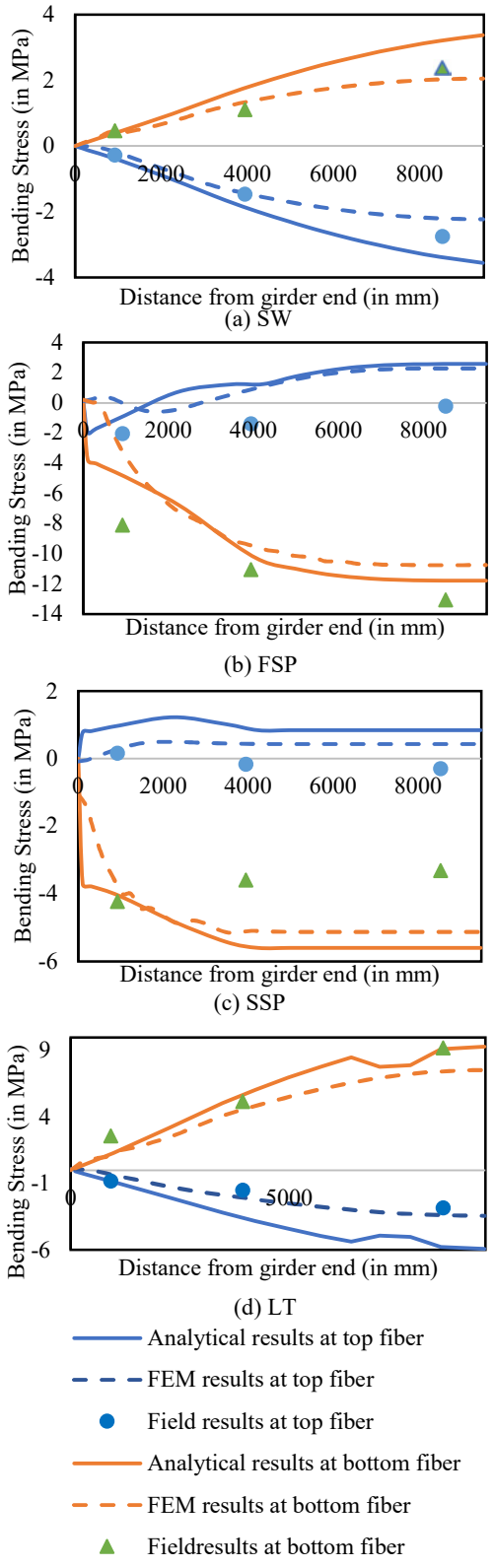

Figure 8 Plot of bending stress at top and bottom fibre along the girder length

4. CONCLUSION

In the present study, 3-D FEM modeling of PSC girders has been done using the commercial software MSC Marc. It has been observed that the structural response of the FE model for midspan displacement, bending stress, and strain is in good agreement with designed values, analytical calculations, and field-instrumented results. Hence the 3D FE model of prestressed girder using thermal load and the INSERT function in the MSC model can be satisfactorily used to simulate the field response of a PSC girder.

The presented modeling technique can be used to evaluate the structural response of a damaged PSC girder due to corrosion. The severity of damage in terms of corrosion level, structural cracks, and concrete section loss can be fed as input, and the reduction in load carrying capacity of a girder can be evaluated. Estimated residual strength can provide a rationale for decision-making regarding the strengthening or decommissioning of a structure.

ACKNOWLEDGEMENT

The authors gratefully acknowledge the support provided by the Indian Railways.

REFERENCES

1) Guidelines for Instrumentation of Bridges, Bridge & Structure Directorate, RDSO, Lucknow, 2016.
2) Choudhary, M. P. and Sanghai, S. S.: Pre-Stressed Concrete Bridge Girder Analysis, Design & Optimization- A Review, International Journal for Research in Applied Science & Engineering technology, vol. 7, no. IV, pp. 1786-1790, 04 2019.
3) Darmawan, M.S. and Stewart, M. G.: Effect of pitting corrosion on capacity of prestressing wires, Magazine of Concrete Research, vol. 59, no. 2, pp. 131-139, 2007.
4) Huang, L.: Finite Element-based Parametric and Probabilistic Analysis of Structural Deterioration in Corroded Pre-stressed Concrete Girders, Alberta, 2020. Barzegar, F. and Maddipudi, S.: Generating Reinforcement in FE Modelling of Concrete Structures, Journal of Structural Engineering, vol. 120, no. 5, 1994.
5) Barzegar, F. and Maddipudi, S.: Generating Reinforcement in FE Modelling of Concrete Structures, Journal of Structural Engineering, vol. 120, no. 5, 1994.
6) Halim, M. . A. and Lebdeh, T. A.: Analytical Study for Concrete Confinement in Tied Columns, Journal of Structural Engineering, vol. 115, no. 11, 1989.
7) Lu, Z. H. and Zhao, Y. G.: Empirical Stress-Strain Model for Unconfined High-Strength Concrete under Uniaxial Compression, Journal of Materials in Civil Engineering, vol. 22, no. 11, 11 2010.
8) Marzouk, H. and Chen, Z. W.: Fracture Energy and Tension Properties of High-Strength Concrete, Journal of Materials in Civil Engineering, vol. 7, no. 2, 1995.
9) Dahmani, L. and Khennane, A.: Modelling and influence of shear retention parameter on the response of reinforced concrete structural elements, Strength of Materials, 2009.
10) Devalapura, R. K. and Tadros, M. K.: Stress-Strain Modelling of 270 ksi Low-Relaxation Prestressing Strands, PCI Journal, vol. 37, no. 2, pp. 100-106, 1992.
11) Motwani, P. and Laskar, A.: Advanced Numerical Simulation technique for Modelling Prestress Transfer, in Proceedings of the 11th Structural Engineering Convention, Kolkata, 2018.